High Temperature Deformation Behavior of Cast Alloy 718

D. Zhao, S. Guillard, and A.T. Male*

Concurrent Technologies Corporation
1450 Scalp Avenue
Johnstown, PA 15904

Abstract

Cast Alloy 718 was evaluated in compression over a range of temperatures (900 to 1120°C), strain rates (0.01 to 1.0 s^{-1}), and true strains (0.15 to 0.7). Under most conditions evaluated, flow curves exhibited no peaks, indicating that dynamic recrystallization was not playing an important role. The percentage of static recrystallization was found to vary with temperature, strain rate, true strain, and time held at temperature after deformation. Recrystallized grain size values were also determined. A material model describing percent recrystallization and recrystallized grain size was established based on the experimental data. In addition, double hit compression tests were conducted to determine the effect of delay time between passes during ingot breakdown. For most cases the percent recrystallization after double hit was simply the sum of two individual hits under corresponding conditions.

This work was conducted by the National Center for Excellence in Metalworking Technology, operated by Concurrent Technologies Corporation under contract No. N00140-92-C-BC49 to the U.S. Navy as part of the U.S. Navy Manufacturing Technology Program.

* Currently with University of Kentucky, Lexington, KY.

Superalloys 718, 625, 706 and Various Derivatives
Edited by E.A. Loria
The Minerals, Metals & Materials Society, 1997

Introduction

Ingot breakdown is the first step in deformation processing of superalloys. The microstructures resulting from this stage influence subsequent microstructure evolution, therefore, the properties of finished components. Moreover, with practical limitation on the diameter of ingot which can be successfully cast and the increasing diameter requirements for some shafts, the billet formed after ingot breakdown is used directly for the shaft with only subsequent heat treatment and machining. It is thus very important to have uniform fine grain microstructure in the forged billets in order to guarantee uniform properties. In the past, most hot deformation studies concentrated on subsequent forging of already wrought billets. Only a few investigations dealt with ingot breakdown processes [1-4].

According to the previous work on ingot breakdown of cast Alloy 718, dynamic recrystallization did not play an important role in the ingot breakdown temperature range (around 1121C and below) [1, 3], except in Garcia's work [4]. A study on wrought Alloy 718 indicated that strain per pass was the most important factor [5]. Accumulated total strain did not significantly affect recrystallization behavior. The specimen size was small for as-cast alloy in most studies because of the load requirement for larger specimens. More systematic testing to determine the percentage and kinetics of recrystallization is needed. The dependence of recrystallization on time, temperature, strain, strain rate, and starting grain size needs to be further investigated.

Material and Test Procedure

The cast Alloy 718 used in this investigation was provided by Inco Alloys International, Huntington, WV. The material was a middle section of a cast ingot. It was subsequently homogenized following a proprietary heat treatment procedure. Figure 1 shows the cast and homogenized macrostructure. The chemical composition of the alloy is listed in Table I.

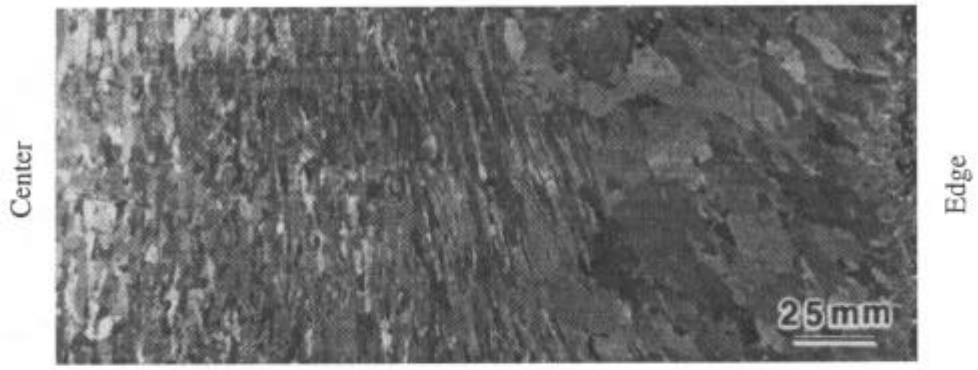

Figure 1 - Homogenized macrostructure of Alloy 718 ingot.

Table I Chemical Composition of Alloy 718 (wt.%, Ni bal.)

C	Fe	Mn	Si	P	S	Cr	Al	Ti	Mg	Mo	Cu	Co	B	Nb
.03	17.81	.08	.10	.011	.001	18.43	.57	.90	.001	3.02	.09	.16	.003	5.30

The grain structure did not change much within the mid-radius, while it was coarser from the mid-radius to the surface. The grain structure was divided into two zones: (A) from near center to 140 mm-radius with finer grains, and (B) from 140 mm-radius to surface with coarser grains.

Compression specimens were 19 mm diameter by 28.5 mm height, which is larger and more representative than most of the previous studies [1-2]. The higher aspect ratio of 1.5 was meant to include more grains in each specimen and to minimize the effect of friction during testing. Grooves were machined at the specimen ends to retain lubricant during deformation. Boron nitride was used as lubricant. The lubricant was brushed on twice to ensure it filled the grooves. Specimens were machined with their axis in a radial direction with respect to the cast ingot for the compression results to be directly applicable to deformation simulation of the breakdown (cogging) operation.

The test conditions chosen were determined by current industrial cogging practice. For Zone A, temperatures were chosen as 1121, 1093, 1066, 1010, 954, and 899°C, strain rates as 0.01, 0.1, and 1.0 s^{-1}, true strains of 0.15 and 0.30 (except for the tests below 1010°C for which 0.5 true strain was used), and hold time of 5, 20, 50, and 100 s (except for the tests below 1010°C where recrystallization does not occur). For Zone B, temperatures were chosen as 1121 and 1066°C, strain rate as 0.1 s^{-1}, true strains of 0.15 and 0.30, and hold time 5, 20, 50, and 100 s.

Most of the specimens were machined from Zone A to include more grains within one specimen than in Zone B and reduce the effect of cast texture to avoid severe nonuniform deformation. Some of the testing conditions were combined for double-hit tests. A computer program was written to conduct double-hit tests with controlled hold time between hits. For all the tests, the specimens were held at the testing temperature for 5 minutes before the compression commenced. Immediately following testing, the specimens were held at temperature for various times to determine the recrystallization behavior. Water quenching was used at the end of the hold time to retain the high temperature microstructures.

Results and Discussions

Flow Behavior

A typical true stress-true strain curve for cast and homogenized Alloy 718 is shown in Figure 2. In most cases, flow stress was relatively constant with respect to strain after initial work hardening, indicating an absence of dynamic recrystallization. This is consistent with the findings of previous work by Weis [1] and DiConza [3]. Softening occurred in a few cases where temperature was low and strain rate was high. This softening was judged to be mainly caused by deformation heating and localized flow. The tendency for softening increased with decreasing temperature and increasing strain rate. The extent of dynamic recrystallization would be expected to increase with increasing temperature so it is probable that the observed softening is not related to dynamic recrystallization. However, at low temperatures and high strain rates (0.1 and 1 s^{-1} at 954°C and 1 s^{-1} at 1010°C), the slope of the stress-strain curves during the initial hardening was low. A similar phenomenon was found in the flow curves presented by Garcia [4]. Because of the presence of friction effect and cast texture, nonuniform deformation did occur. This nonuniform deformation not only affected the flow stress after the maximum stress was reached, but also decreased the initial work hardening slope of the stress-strain curves. In some cases, it caused the flow stress to be lower at higher strain rate than at lower strain rate during initial hardening. For the same reason, flow stress could be lower at a lower temperature than at a higher temperature as shown in a previous study [4].

A flow curve for a specimen taken from Zone B of the cast and homogenized Alloy 718 ingot is also shown in Figure 2. The flow behavior was similar to that from Zone A under the same

testing condition, 1066°C and 0.1 s^{-1}. The flow stress was slightly higher because of the larger grain size in Zone B, consistent with a previous study [2].

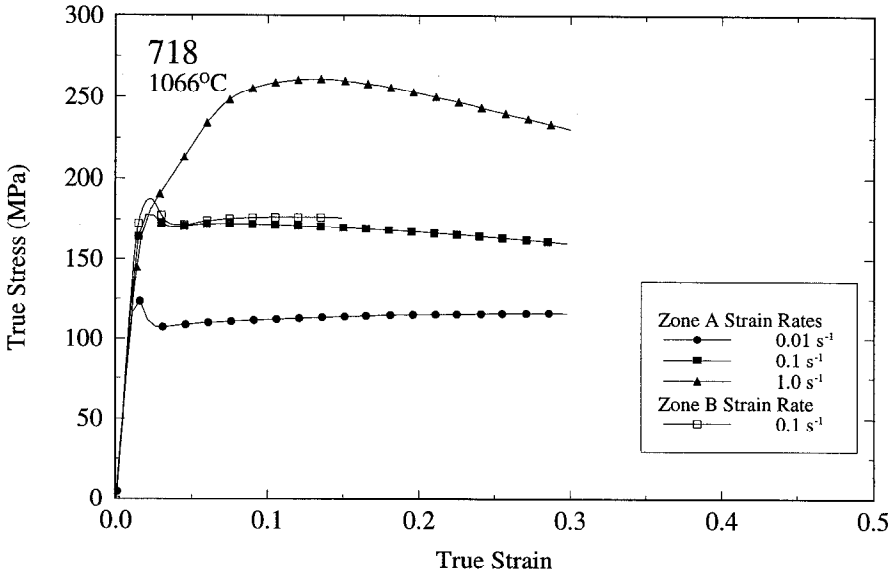

Figure 2 - True stress-true strain curves of cast and homogenized Alloy 718 at 1066 °C.

Figures 3 and 4 show that in double hit tests, the extent of softening was a direct function of holding time between the hits. As holding time was increased, the percentage recrystallization increased, as shown in the next section, and the amount of softening increased.

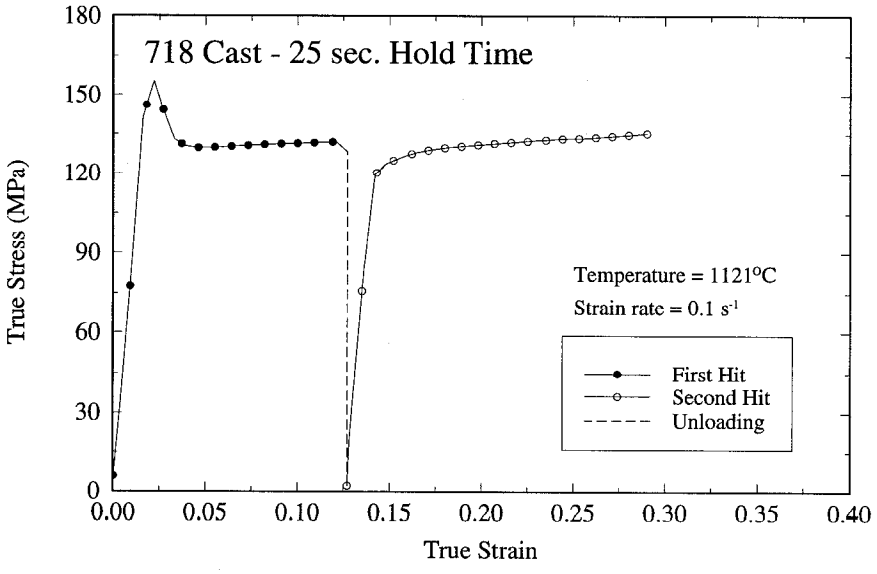

Figure 3 - True stress-true strain curve of cast and homogenized Alloy 718 for double hit test, 1121°C and 0.1 s^{-1}, holding time between hits 25 s.

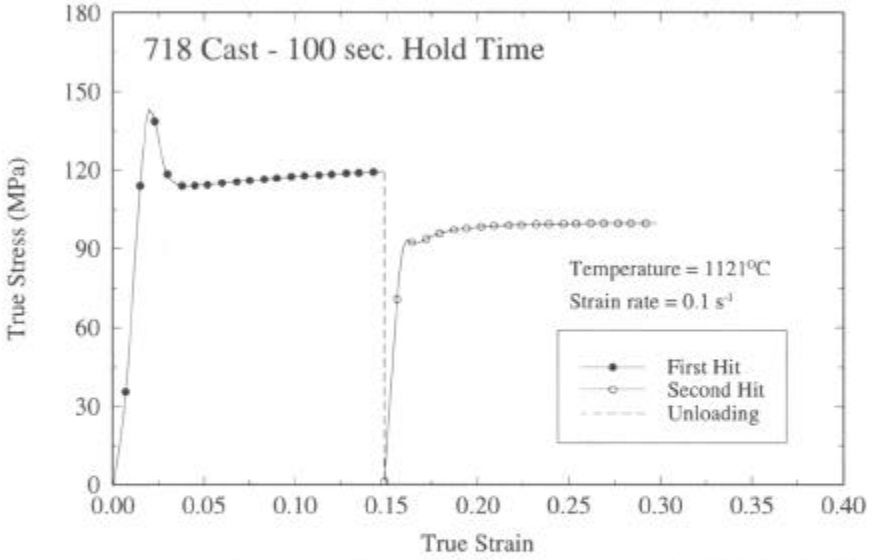

Figure 4 - True stress-true strain curve of cast and homogenized Alloy 718 for double hit test, 1121°C and 0.1 s^{-1}, holding time between hits 100 s.

Microstructure Evolution

The starting cast and homogenized microstructure is shown in Figure 5. After homogenization, the Laves phase and δ-phase disappeared, indicating effective homogenization treatment. The large particles are M(C,N) type. Energy dispersive x-ray (EDX) showed the particles are mainly Nb rich with some Ti.

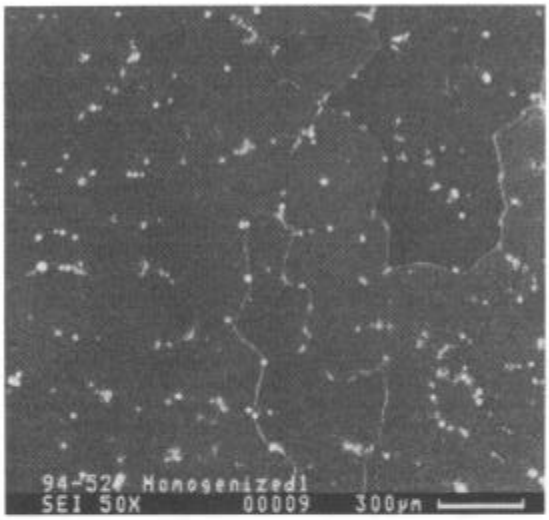

Figure 5 - SEM micrograph showing homogenized microstructure of cast and homogenized Alloy 718.

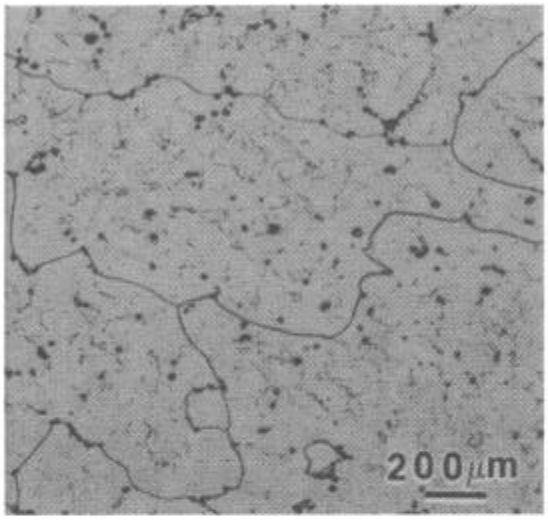

Figure 6 - Optical micrograph of deformed Alloy 718 (Zone A), showing recovery 1010°C, 0.01 s^{-1}, true strain 0.15, and holding time 20 s.

In the deformed specimens, recovery and recrystallization were observed, depending on testing conditions. Figure 6 shows that at a temperature of 1010°C, strain rate 0.01 s^{-1}, true strain 0.15, and hold time 20 seconds, the microstructure had recovered; etch pits and precipitates show formation of dislocation substructures, an indication of recovery. At this condition, the

temperature and the amount of input energy were not sufficiently high to cause recrystallization. Figure 7 shows the initial stage of recrystallization at 1166°C, 0.01 s^{-1}, 0.3 true strain, and 100 second hold time. The nucleation started around the particles and at the grain boundaries. In general, the recrystallization sites were mostly around particles, because of the scarcity of original grain boundaries. In most cases, the original grain boundaries are still visible after recrystallization. The high dislocation density around the particles and original grain boundaries helped the formation of new grains. The nucleation of new grains did not always utilize the original grain boundaries or the interfaces between the particles and the matrix as one boundary of the new grains. The nucleation mechanism of subgrain rotation proposed by Li [7] was at least partially responsible for the present recrystallization. At 1121°C, 0.1 s^{-1}, 0.3 true strain, and 100 second hold time, the microstructure was almost completely recrystallized, as shown in Figure 8.

Microstructural analysis of the specimens taken from Zone B showed similar behavior as those from Zone A in terms of amount of recrystallization and recrystallized grain size. The main reason for the similar recrystallization behavior was that grain boundaries were limited in the specimens from either zone, but the number of particles were comparable to provide a similar number of nucleation sites.

For double hit tests, the amount of recrystallization was not equal to that of a specimen with the same total strain achieved through a single hit at the same temperature and holding time conditions. However, it was approximately the same as the sum of two separate specimens experiencing a single hit. For example, a specimen hit with 0.15 strain+100 s hold, and then another 0.15 strain+100 s hold would have similar percent recrystallization as the sum of percent recrystallization as one specimen hit with 0.15 strain+100 s hold and another specimen hit with 0.15 strain+100 s hold.

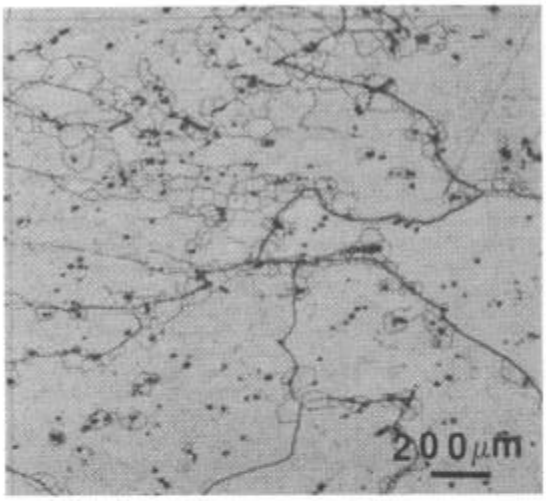

Figure 7 - Optical micrograph of deformed Alloy 718 (Zone A), showing onset of recrystallization, 1066°C, 0.01 s^{-1}, true strain 0.3, and holding time 100 s.

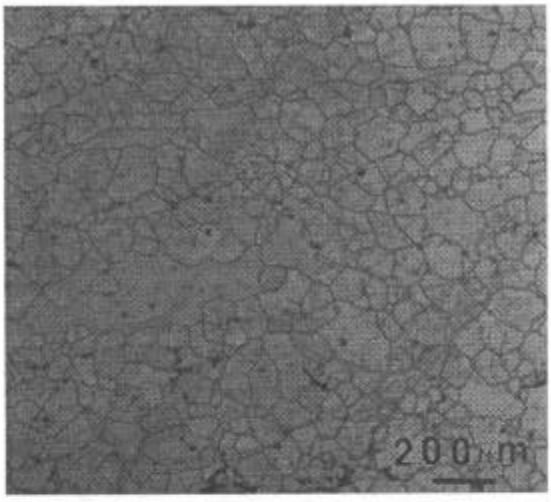

Figure 8 - Optical micrograph of deformed Alloy 718 (Zone A), showing almost complete recrystallization 1121°C, 0.1 s^{-1}, true strain 0.3, and holding time 100 s.

In the center region of the deformed specimens, the amount of recrystallization was higher than at the other locations of the specimen. Since the deformation of the specimens was not uniform because of the friction, barreling did occur. A finite element analysis was conducted to estimate the equivalent strain in the center region of the specimen. The actual strain was 0.2 for a nominal strain of 0.15, and 0.4 for a nominal strain of 0.3. To systematically measure

the microstructural features, five pictures at 50X were taken in the central region of each specimen.

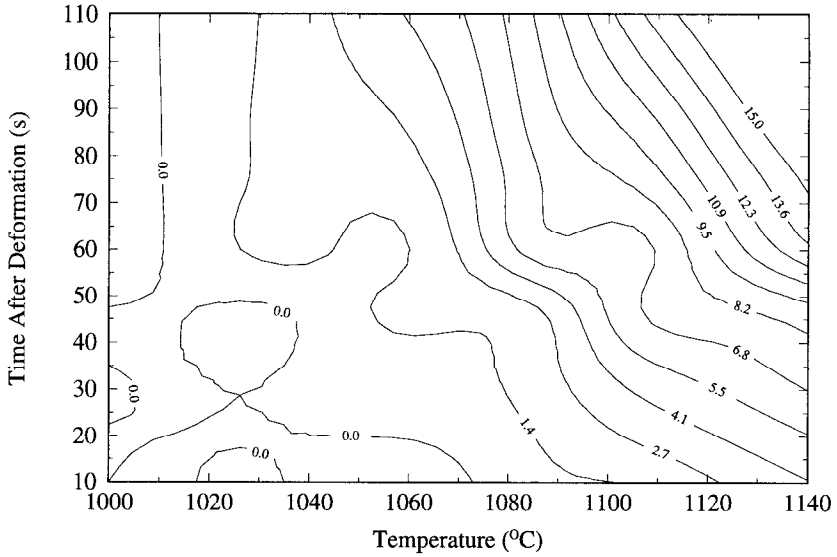

Figure 9 - Percent recrystallization at 0.15 nominal strain (0.2 strain at the center of the specimen) and a strain rate of 0.01 s^{-1}.

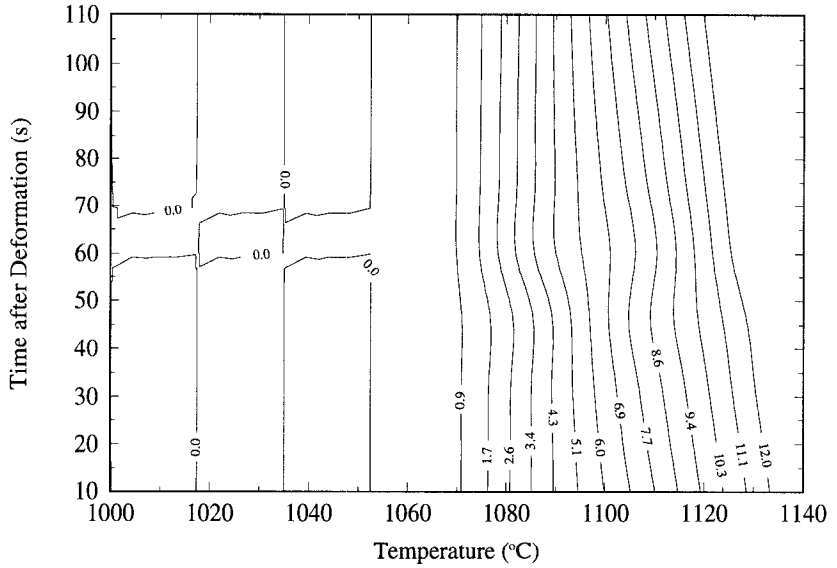

Figure 10 - Percent recrystallization at 0.15 nominal strain (0.2 strain at the center of the specimen) and a strain rate of 0.1 s-1.

At temperatures 1010°C and below, the percent recrystallization was small. To determine whether this would also be the situation at large strains, a few tests were run to a nominal strain of 0.7. The microstructural analysis showed that the maximum percent recrystallization was 14% after 0.7 true strain and 100 second hold, which was still not significant. Cogging at these temperatures will not produce massive recrystallization in the workpiece. However, recrystallization during reheating is extensive. A two and one half hour reheating at 1041°C resulted in complete recrystallization for the specimens deformed at 1010°C.

Figures 9 through 11 show the percent of recrystallization as a function of temperature and holding time for the specimens deformed to a nominal strain of 0.15 (local strain of 0.2 at the center of the specimens). The percent recrystallization was mainly affected by temperature. The holding time had some effect on the amount of recrystallization at the lowest strain rate 0.01 s^{-1}, but little effect at strain rates 0.1 and 1.0 s^{-1}. The percent recrystallization was relatively low at this true strain, with the maximum being 16%. The effect of strain rate was weak. Figures 12 through 14 show the percent recrystallization for the specimens deformed to a nominal strain of 0.3 (local strain of 0.4 at the center of the specimens). Although the temperature effect was still important, the effect of holding time was also intensified, and the effect of strain rate was strong between 0.01 s^{-1} and 0.1 s^{-1}, and became weaker between 0.1 s^{-1} and 1.0 s^{-1}. The maximum percent of recrystallization was as high as 87%.

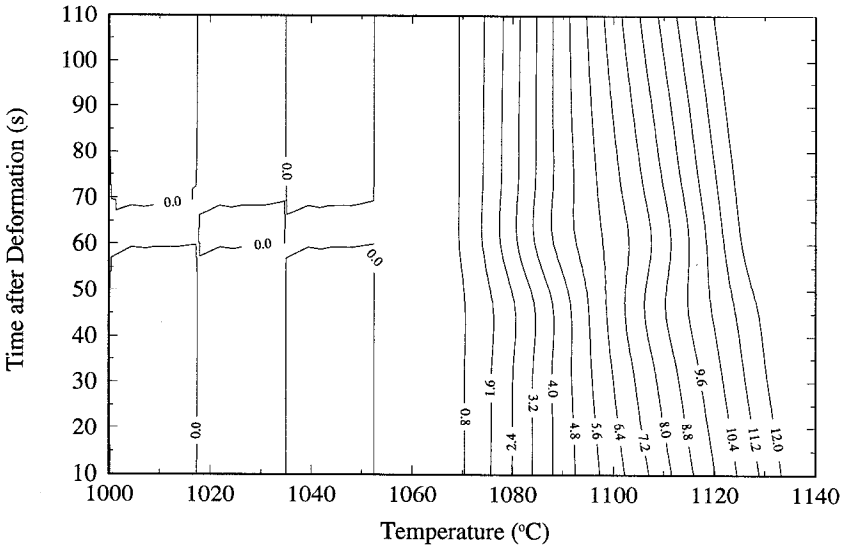

Figure 11 - Percent recrystallization at 0.15 nominal strain (0.2 strain at the center of the specimen) and a strain rate of 1.0 s^{-1}.

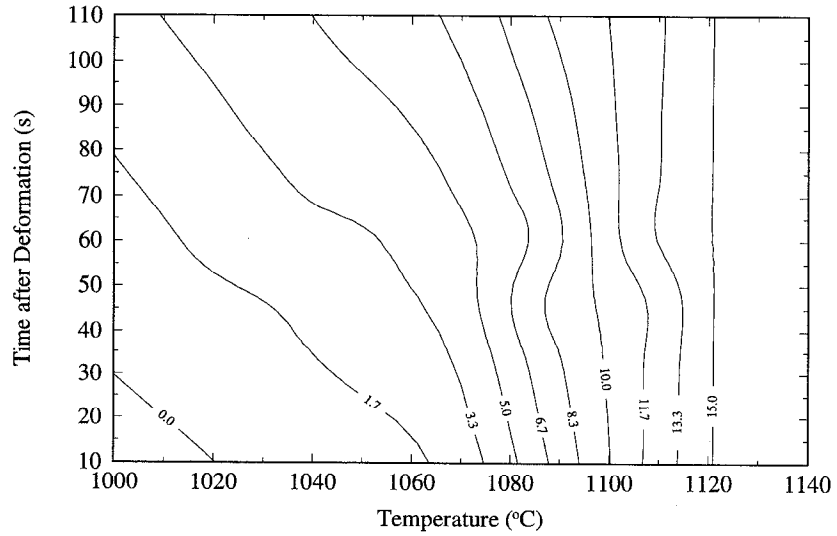

Figure 12 - Percent recrystallization at 0.3 nominal strain (0.4 strain at the center of the specimen) and a strain rate of 0.01 s^{-1}.

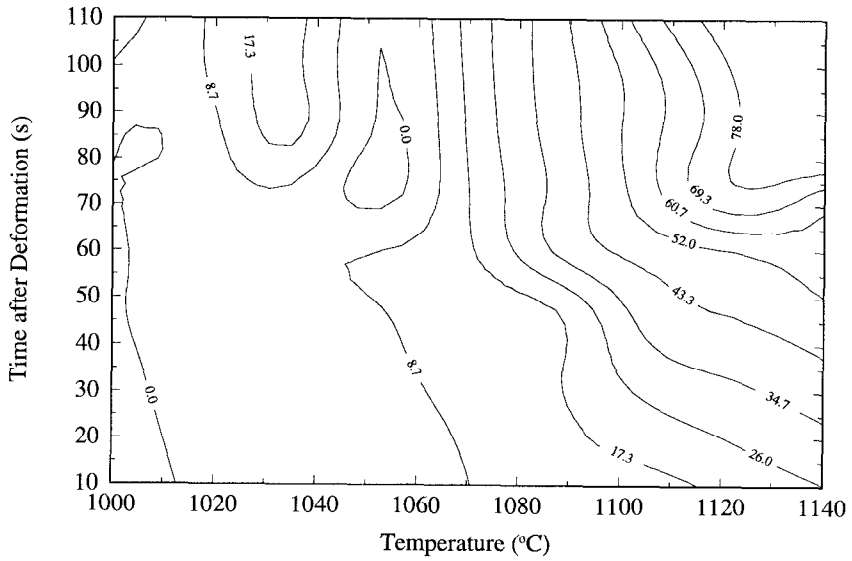

Figure 13 - Percent recrystallization at 0.3 nominal strain (0.4 strain at the center of the specimen) and a strain rate of 0.1 s^{-1}.

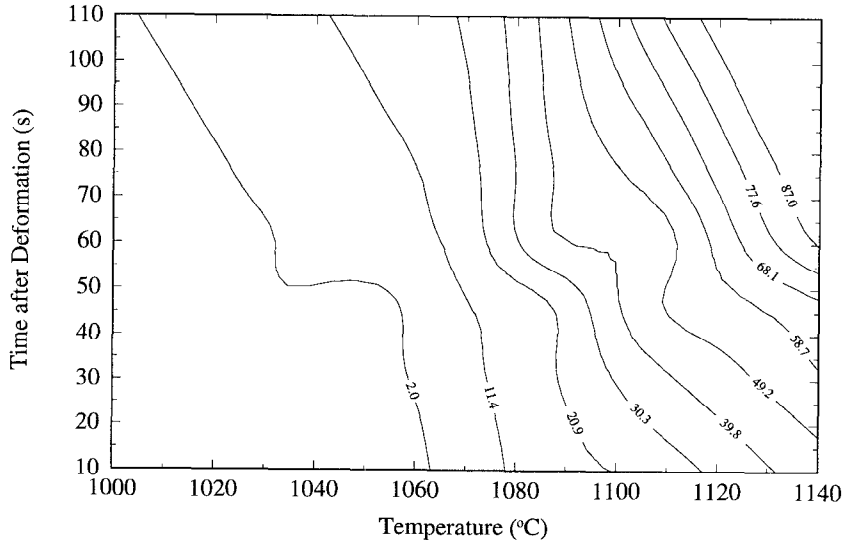

Figure 14 - Percent recrystallization at 0.3 nominal strain (0.4 strain at the center of the specimen) and a strain rate of 1.0 s^{-1}.

Figure 15 shows recrystallized grain size at 0.3 nominal strain (0.4 strain at the center of the specimen) and a strain rate of 0.1 s^{-1}. The recrystallized grain size was dependent on both temperature and hold time. However, the effect of amount of deformation and strain rate did not appear significant on the recrystallized grain size, as shown in Figure 16.

The preceding results were used to derive a semi-empirically based model expressing the percentage of static recrystallization and the size of the statically recrystallized grains. The chosen form to express the percentage of static recrystallization was

$$X = 1 - \exp\left[-0.693\left(\frac{t}{t_{0.5}}\right)^{n_a}\right] \qquad (1)$$

where t is the time the material is held at temperature, $t_{0.5}$ is the time needed at that temperature to achieve 50% recrystallization, and n_a is a material constant.

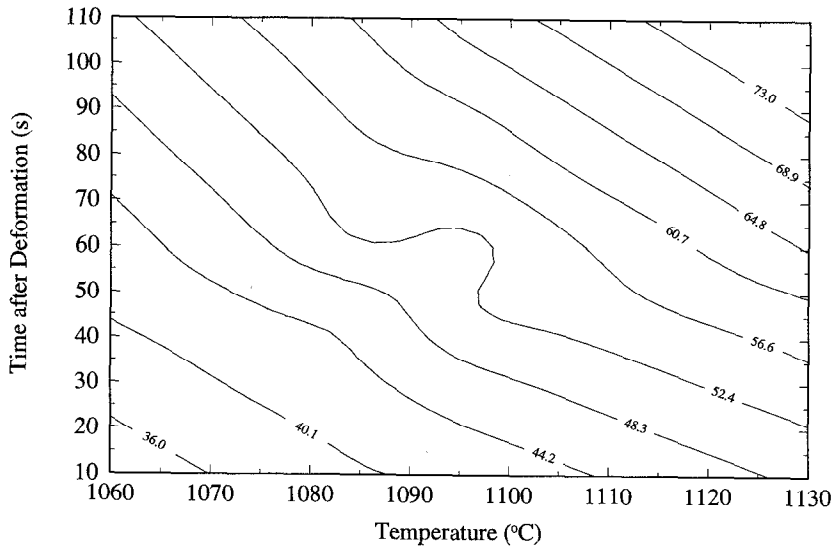

Figure 15 - Recrystallized grain size at 0.3 nominal strain (0.4 strain at the center of the specimen) and a strain rate of 0.1 s^{-1}.

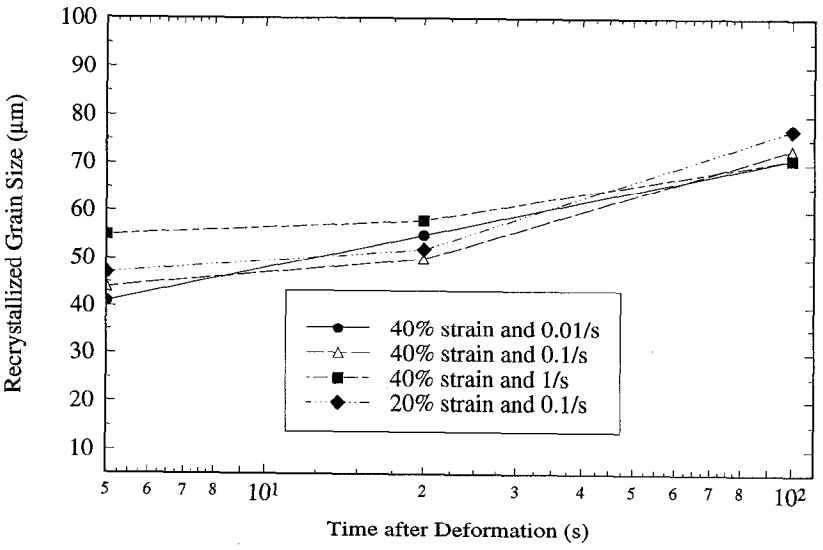

Figure 16 - Recrystallized grain size at 1121°C and various strains and strain rates.

Plots of $ln[ln(1/(1-X))]$ versus $ln\ t$ were obtained to determine the values of $t_{0.5}$ and of n_a. The value of n_a was not a constant and had to be expressed as a function of strain and temperature. Similarly, whereas an Arrhenius-type relationship was expected for $t_{0.5}$, the constant in that relation was found to vary with strain and temperature. The quantity $t_{0.5}$ (must be equal or greater than 20 seconds) was therefore expressed as a function of temperature and strain, using the best possible fit of the experimental data. The obtained expressions are

$$t_{0.5} = \frac{9.777\text{x}10^{8}}{T} - \frac{4.78\text{x}10^{3}}{\varepsilon} + \frac{2.8159\text{x}10^{7}}{\varepsilon T} - 7.2936\text{x}10^{5} \qquad (2)$$

$$n_a = 0.3 - 0.0012t + (\varepsilon - 0.26)(\varepsilon - 1.15)\left[\frac{t}{35} - |1366 - T|(0.0012(t-6) + 4\text{x}10^{-5}|1339 - T|t - 50|)\right]$$

for $T \geq 1339\text{K}$ and with $n_a \geq -0.1$ (3)

$n_a = 0.3$ for $T < 1339\text{K}$.

The model was derived using the experimental data at 1066 and 1121°C. Figure 17a shows how the predicted percentages of static recrystallization (SRX) compare with the experimentally measured values at those two temperatures, which represent the bounds of the model validity. Agreement between predictions and measurements is very good at the lower temperatures for all holding times, and at the higher temperatures for holding times between one and two minutes. The model should not be used for holding times longer than two minutes. This is appropriate for the cogging simulation for which the holding time between two successive hits in any given location is less than approximately 2 minutes. The size of the recrystallized grains was found to fit the following equation:

$$d = A\left(\frac{T}{1223}\right)^{3} \exp\left[3\text{x}10^{-5}\ (T\ -\ 1223\ )\ t\right] \qquad (4)$$

where d is in μm, and the value of A is between 25 and 34. The above equation reflects the fact that, as presented earlier, neither strain nor strain rate were found to significantly influence grain size. Figure 17b shows that the model predictions are very reasonable when compared to the experimental results (solid symbols).

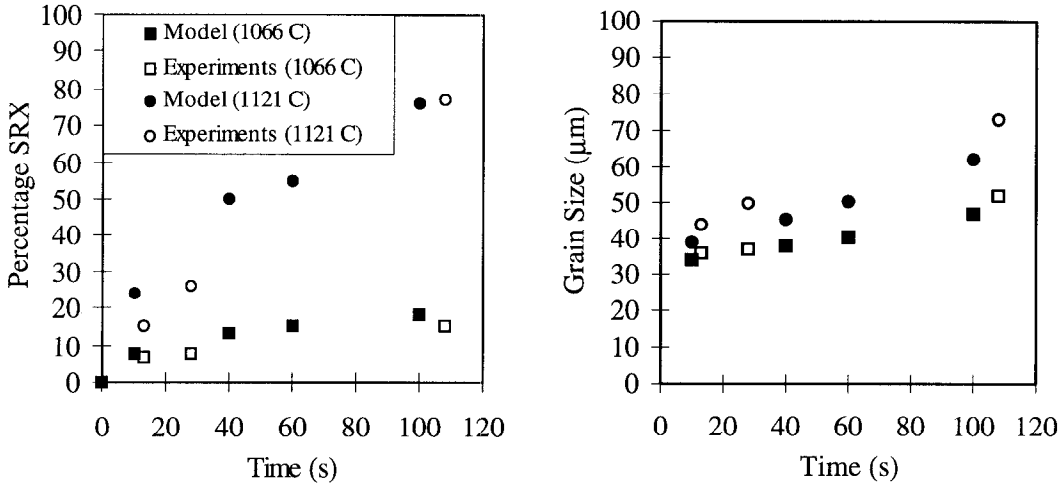

(a) (b)

Figure 17 - (a) The predicted percent static recrystallization (SRX) and, (b) the predicted size of statically recrystallized grains compared with the experimentally measured values at 1066°C and 1121°C, strain 0.3.

Summary and Conclusions

The flow behavior and microstructural evolution of cast and homogenized Alloy 718 were investigated by conducting compression tests over a range of temperatures, strain rates, and holding times. The following conclusions can be drawn from this work:

The flow stress of cast and homogenized Alloy 718 is relatively constant after initial work hardening. It is an indication that dynamic recrystallization is not significant. The flow stress is not affected significantly by the grain size. Larger grain size at the outer part of the ingot results in slightly higher flow stress.

Static recrystallization is dominant in cast and homogenized Alloy 718 over the temperature (899 to 1121°C) and strain rate (0.01 to 1.0 s^{-1}) ranges commonly used in cogging. At temperatures 1010°C and below, the amount of recrystallization is not significant after deformation, but can be significant after prolonged reheating at a temperature higher than 1010°C. The recrystallization occurred mainly at precipitate particles and prior grain boundaries. Because of the scarcity of prior grain boundaries, the recrystallization at precipitate particles was the main recrystallization mechanism. This diminished the effect of prior grain size on recrystallization.

The amount of recrystallization was mainly affected by temperature at a lower true strain such as 0.2. The holding time had some effect on the amount of recrystallization at the lowest strain rate 0.01 s^{-1}, but little effect at strain rates 0.1 and 1.0 s^{-1}. The effect of strain rate was weak. However, at a true strain of 0.4, although the temperature effect was still important, the effect of holding time was also intensified, and the effect of strain rate was strong between 0.01 and 0.1 s^{-1}, and became weaker between 0.1 and 1 s^{-1}. The recrystallized grain size was dependent on both temperature and hold time. However, the effect of amount of deformation and strain rate did not appear significant on the recrystallized grain size.

In double hit tests, the amount of recrystallization was not equal to that of a specimen with the same total strain achieved through a single hit at the same temperature and holding time conditions. However, it was approximately the same as the sum of two separate specimens experiencing a single hit.

References

1. M.J. Weis et al., "The Hot Deformation Behavior of an As-Cast Alloy 718 Ingot," Alloy 718 - Metallurgy and Applications , ed. E.A. Loria (Warrendale, PA: TMS, 1989), 135-154.

2. M.C. Mataya et al., "Grain Refinement During Primary Breakdown of Alloy 718," 1987 Mechanical Working and Steel Processing Proceedings, (Warrendale, PA: ISS, 1987), 235-247.

3. P.J. DiConza, R.R. Biederman, and R.P. Singh, "Homogenization and Thermomechanical Processing of Cast Alloy 718," Superalloys 718, 625 and Various Derivatives, ed. E.A. Loria (Warrendale, PA: TMS, 1991), 161-171.

4. C.I. Garcia et al., "Microstructural Refinement of As-Cast Alloy 718 via Thermomechanical Processing," *ibid*, 925-941.

5. J. Domblensky et al., "Prediction of Grain Size During Multiple Pass Radial Forging of Alloy 718," Superalloys 718, 625, 706 and Various Derivatives, ed. E.A. Loria (Warrendale, PA: TMS, 1994), 263-272.

6. A. Laasraoui and J.J. Jonas: "Recrystallization of Austenite after Deformation at High Temperatures and Strain Rates - Analysis and Modeling", Metall. Trans. A, 22A (1991), 151-160.

7. J.C.M. Li, J. Appl. Phys., 33 (1962), p. 2958.